Grzegorz KŁOSOWSKI[*], *Tomasz KLEPKA*[**],
Agnieszka NOWACKA[**]

NEURAL CONTROLLER FOR THE SELECTION OF RECYCLED COMPONENTS IN POLYMER-GYPSY MORTARS

Abstract

This study presents research on the development of an intelligent controller that allows optimal selection of rubber granules, as an admixture recycling component for polymer-gypsy mortars. Based on the results of actual measurements, neural networks capable of predicting the setting time of gypsum mortar, as well as determining the bending and compressive strength coefficients were trained. A number of simulation experiments were carried out, thanks to which the characteristics of setting times and strength of mortars containing different compositions of recycling additives were determined. Thanks to the obtained results, it was possible to select the rubber admixtures optimally both in terms of the percentage share as well as in relation to the diameter of the granules.

1. INTRODUCTION

This paper presents the original method of selecting the amount of admixture of rubber granulate and the diameter of granules for the gypsum mixture. Thanks to the use of artificial neural networks, a neural controller has been developed that allows optimal selection of gypsum mixture parameters. Three output variables were optimized: setting time [min], bending strength coefficient (BSC) and compressive strength coefficient (CSC).

---

[*] Lublin University of Technology, Lublin, Poland, +48 81 538 45 67, g.klosowski@pollub.pl
[**] LUT – Department of Technology and Polymer Processing, Lublin, Poland, +48 81 538 47 66

Calcium sulphates in semi-aquatic form have been used for a long time as building binding materials, so-called gypsum binders (Osiecka, 2005). These binders are ecological materials, obtained from natural raw materials, which allow building elements of various sizes and shapes to be quickly and easily (Chłądzyński, 2008). Modern binders are increasingly being created by adding ingredients in the form of fillers from various materials (Hooton, 2015). Due to the size of production and the possibility of processing into valuable building materials, materials originating from waste are becoming more and more important as binder additives, among which the ones of polymer materials are of the greatest importance (Di Mundo, Petrella & Notarnicola, 2018). The basic advantage which should have a new gypsum binder containing a semi-hydrate, deciding its usefulness in construction, is the short setting time and obtaining a good hardness (Serna, del Rio, Palomo & González, 2012). The binder can thus be a polymer-mineral mixture (polymer-cement or gypsum and polymer-lime) as well as a mortar with the addition of only polymer fillers (Aslani, Ma, Wan & Muselin, 2018).

In construction mobile connections, which include expansion joints and larger assembly gaps, the joint material must provide adjacent structures with the possibility of mutual movement in a specific plane, with a clearly defined range of changes (Claudiu, 2013). The vibrations of load-bearing elements, caused by external loads, e.g. shocks, uneven settlement of objects, dynamic loads from vehicle traffic, as well as dimensional changes caused by temperature changes must also be compensated. The sealing materials must therefore have appropriate physical and chemical properties as well as resistance to bending, compressive and shearing forces (Pedro, De Brito & Veiga, 2012). Gypsum-polymer mortars suitable as a binder can work well with virtually all other building materials.

Nowadays, the most pursued route to enhanced elastic properties is the formation of C-S-H organic hybrids on the nanoscale by incorporating soft matter into and/or in between the C-S-H nanoplates (Bergström, 2015; Seto 2012). The two necessary main features for achieving strong specific C-S-H/polymer interactions are negatively charged groups for Ca^{2+} mediated electrostatic interactions and hydrophilic residues preferentially with alcohol or amide groups for hydrogen bond interactions (Picker, 2017). The bond between the C-S-H nanoplates and polymers can be obtained by mixing a resin with aggregate (Kou & Poon, 2013). The most commonly used resins for PC are unsaturated polyester resin, epoxy resin, furan resin, polyurethane resin, and urea formaldehyde resin (Gorninski, 2017). The matrix is given by the polymer which acts as binder of the components, that can be different types of natural aggregates, powders, fibers, nano-materials, etc. (Sosoi & Barbuta, 2018). Polymers, such as styrene-butadiene rubber (SBR) latex and polyvinyl acetate (PVA) emulsion have been commonly used as admixtures in concrete practice (Konar, Das, Gupta & Saha, 2011). This polymer admixtures are known to not only increase the workability but also modify the physical properties of cement pastes by reducing macro voids and improving

the bond strength of the polymer cement mortars to aggregates (Al Menhosh, Wang, Wang, & Augusthus-Nelson, 2018). Recent studies on recycled tire polymer fibers (RTPF) have shown that the addition of this type of fibers in fresh concrete mixes has a positive effect on volume deformations at an early age and mitigates the explosive spalling at high temperatures without affecting the residual mechanical properties of concrete (Baricevic, Jelcic, Rukavina & Pezer, 2018). Based on non-destructive tests (NDT), it was found that increasing the coarse aggregate size and polymer ratio reduced the porosity of specimens. This is attributed to the decreased surface area to volume ratio with increasing particle size, which allowed the polymer to completely coat the surface of aggregates (Jafari, Tabatabaeian & Joshaghani, 2018). However, prior to their utilization in construction products, such materials require characterization which will demonstrate their properties and assure positive long-term behavior, especially when exposed to aggressive environmental conditions (Serdar, 2015).

Such environmental factors could lead to a decrease in performance, thus decrease the durability of concrete. Exposure to high temperatures is one of these physical factors that have an impact on concrete (Sahmaran, 2009). Recent studies shown that structures exposed to high temperature can be used the polymer-phosphazene concrete. The filling of the voids with the polymer was ensured so that the physical binding of polymer molecules and strong adhesion of these molecules to each other was obtained (Tanyildizi & Asilturk, 2018). This strategy could greatly benefit future construction processes because fracture toughness and elasticity of brittle cementitious materials can be largely enhanced on the nanoscale.

Gypsum-polymer mortars can be used to supplement cavities, leveling walls and floors by increasing the elasticity of the mixture (Forrest, 2014). Thanks to this, after solidifying, the weld section made is resistant to deformation that occurs during the period of operation of the analyzed object (Benosman et al., 2017). Gypsum-polymer mortar can be products with good functional properties, easy to use. Proper selection of the additive, e.g. regranulate, will allow to obtain an improved flexible mortar, which can be evaluated on the basis of tests of bending strength or compressive strength, etc. (Jarosiński, Żelazny & Nowak, 2007; Herrero, Mayor & Hernández-Olivares, 2013).

The aim of the research was to develop an intelligent controller that would allow optimal selection of rubber granulate parameters as an admixture for gypsum-polymer mortar with addition of hydrated lime and admixtures in various amounts from rubber regranulate. Parameters such as: time of setting components of the gypsum mixture (minimization of time) and mechanical properties of the obtained mortar (maximization of strength) were optimized.

2. MATERIALS AND METHODS

During the research it was found that due to the complex, non-linear dependence of 2 independent variables (input):

1. Diameter of granules,
2. Percent of admixture,

regressive neural networks can be an appropriate tool to train the controller (Lorrentz, 2015). Based on 120 real measurements, 3 separate neural networks were trained. Each of the networks had at the entry 2 of the above-mentioned values. The network outputs were: setting time [min], bending strength factor (BSC) and compressive strength index (CSC). Both strength coefficients are expressed in Newton [N].

In order to collect training data for the neural network, research was conducted on polymer-gypsum mortars. The tests were based on samples similar in shape and size to welds used in real conditions. Characteristic indicators that determined the weld's usefulness are the time of binding of the gypsum-polymer mixture as well as the bending and compression strength factors.

$CaSO_4 \cdot \frac{1}{2}H_2O$ construction gypsum was used for the developed material composition. The gypsum bond fulfilled the requirements of EN 13279-1-A1. The content of calcium sulphate ($CaSO_4$) was above 50%, the graining of the material was covered by a 1.0 mm sieve residue, no more than 0.5% and a 0.2 mm sieve, which was equal to or lower than 15%. Hydrated lime was added to the mixture, its share in mixtures with gypsum did not exceed 2%. Rubber granulate derived from the recycling of tires with several grain diameters from ø 0.1 mm to ø 0.63 mm was used as an additive to increase flexibility.

The components of the mixtures were introduced in various proportions to the binder when mixing with water. They consisted of gypsum, hydrated lime and polymer regranules. When choosing the right regranulate for the tests, the amount of polymer incorporated into the mixture was also significant, the appropriate amount being determined based on the adopted research program.

Fig. 1 presents molds for the preparation of gypsum-polymer mortar beams. Fig. 2 presents a sample of a set plaster mortar containing 20% of a rubber granulate with a granule diameter of 0.1 mm.
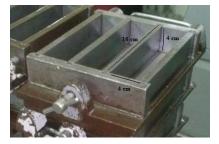

Fig. 1. Molds for the preparation of mortar beams

Fig. 2. Gypsum mix with 20% rubber granulate with a grain diameter of ⌀ 0.1 mm

To determine the bending and compressive strength of the samples, a hydraulic press with a 16 cm^2 jaw area was used, compressing at the standard speed, with a jaw pressure from 0–200 kN. The studies of setting time of gypsum mixtures were made using the Vicat apparatus.

Fig. 3 shows a schematic of a neural network. The input vector consists of 2 elements. It is a multi-layer perceptron with one hidden layer containing 10 neurons (Thomas & Thomas, 2011). The hidden layer transition function has a sigmoidal waveform. One neuron is located in the output layer. The transition function has a linear course here. The output is a real number, so we are dealing with a regression model.
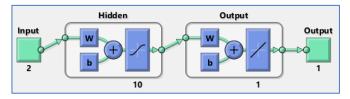

Fig. 3. Diagram of neural network used in research

Table 1 shows the results of training the neural network. The historical data set consisted of 120 cases, divided into 3 sets: training set, validation set and testing set, in the ratio of 70:15:15. The main measures of network quality are mean squared error (MSE) and regression (R).

Tab. 1. Results of neural network training for individual sets

Sets	Samples	MSE	R
Training	84	$6.51330 \cdot 10^{-4}$	0.997353
Validation	18	$1.66109 \cdot 10^{-3}$	0.994454
Testing	18	$5.97817 \cdot 10^{-4}$	0.998574

The formula based on which the MSE error is calculated is presented using the dependence (1).

$$MSE = \frac{1}{n} \cdot \sum_{i=1}^{n} (ref_i - x_i)^2 \tag{1}$$

where: n – number of cases in the set (training, validating or testing),
         ref – reference values (patterns),
         x – predicted values of a model.

The high quality of the network is demonstrated by low MSE and high R. The best indicator reflecting the ability of the neural network for generalization is MSE for testing set. Testing set contains cases that did not participate in the network training process, hence MSE for testing set is usually higher than for training set. In the present case, the MSE values for testing set and training set are very similar. Both values are very low, which is a good sign of the quality of the trained neural network. Regression for testing set is 9.986 which is a high indicator and also confirms the effectiveness of the solution obtained.
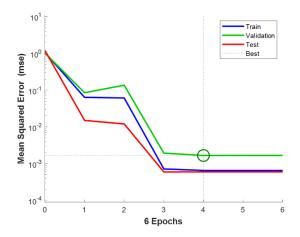

Fig. 4. Plot of neural network performance according to MSE

Fig. 4 shows the course of training the neural network based on the MSE values in individual iterations (epochs). The shape of the curve resembles a bit of hyperbole.
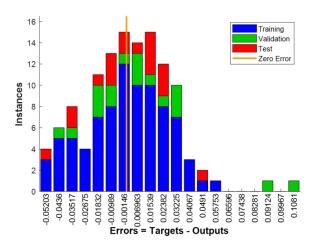
53

Fig. 5. Error histogram of the neural network training process

There are not many fluctuations on the chart. These features testify to the lack of network overtraining. On the line of the validation error, the place where the learning process ends was marked. It falls into epoch 4. Best validation performance (MSE) equals 0.0016611. The task of the validation set is to stop training the neural network, which occurs when after six successive iterations MSE does not fall.

Fig. 5 shows a histogram of MSE errors for sets: training, validation and testing. The whole range of errors has been divided into 20 bins. The most errors had absolute values close to zero. The shape of the graph resembles a normal distribution curve, which also well shows the quality of the obtained neural network.

Quantitatively, the most registered MSE errors concerned training set. This is due to the fact that all historical cases were divided in such a way that as many as 70% of them fell on the test set. The remaining 30% were divided into validation and test sets. Fig. 5 reflects this division.

Fig. 6 presents regression statistics of the obtained neural network. As you can see, regression is close to 1 for both the test set (left picture) and for all cases including training, validation and testing (right picture).

Regression is a measure of matching the network response to patterns. If it is close to 1 even for test cases that do not participate in the network learning process, it means that the network has the ability to generalize responses. This is a key feature thanks to which the network deserves to be called intelligent.
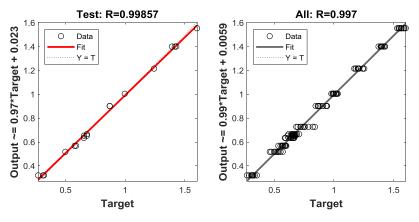
54

Fig. 6. Regression statistics of the neural network training process

Fig. 7 shows a simulation model of the system for the selection of recycled components in polymer-gypsy mortars. The configuration of the presented model assumes that the diameter of the rubber granulate is constant and amounts to ⌀ 0.35 mm. The percentage of admixture varies in the given range. Several variants of simulation models were tested, in which the constant diameter of granules assumed the following values: ⌀ 0.1, 0.2, 0.35 and 0.5 mm. For each given diameter of granules, the percentage of admixture was smoothly changed.
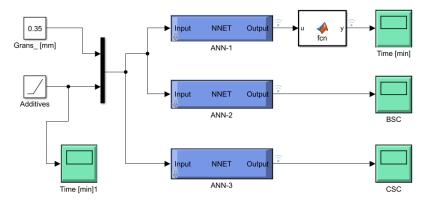

Fig. 7. Simulation model including three separate neural networks

Three separate neural networks were trained in which each had a different output. In the first network (ANN-1) the dependent variable was the binding time, in the second network (ANN-2) it was the bending strength factor (BSC) and in the third network (ANN-3) the bending strength index (CSC). In the case of ANN-1 it was necessary to convert the real number to minutes, hence an additional module visible in Fig. 7 was placed to the right of ANN-1.

3. RESULTS

Based on the designed neural models, a number of simulation experiments were carried out, including various variants of intelligent controller settings. Variants were tested in which the diameter of the granules was predetermined (ø 0.1 mm, ø 0.2 mm etc.), while the proportion of admixture of rubber granulate was smoothly variable. The results of the tests are shown in Fig. 8 and Fig. 9.

The drawings are presented in pairs, in a system allowing to compare two cases together with different diameter of granules next to each other with a smooth change in the amount of additives. In Fig. 8, the diameters of granules ø 0.1 mm and ø 0.2 mm were compared. The first pair of graphs in Fig. 8 shows the duration of the binding time expressed in minutes. The next pairs of drawings show the waveforms of BSC and CSC values expressed in Newtons. The drawings in Fig. 9 are presented in an analogous manner, but the analyzed cases concerned different granule diameters: ø 0.35 mm and ø 0.5 mm.
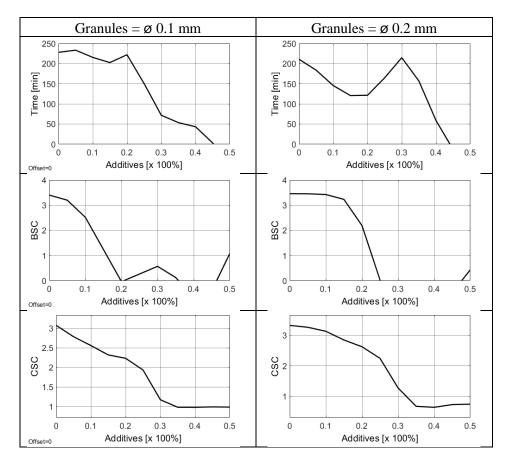

Fig. 8. Prediction results with constant granule diameters (Ø 0.1 mm and Ø 0.5 mm)
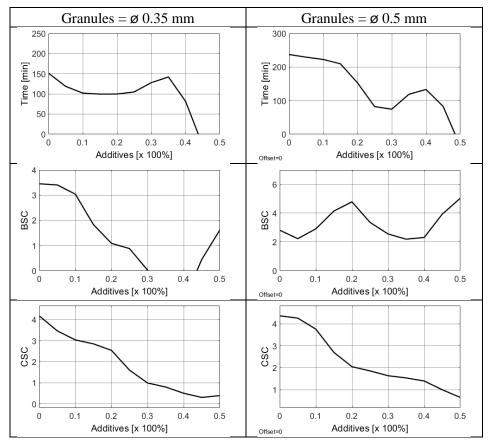
56

Fig. 9. Prediction results with constant percentage inclusions (10% and 40%)

4. CONCLUSIONS

Analyzing the results of the experiments shown in Figs. 8 and 9, it can be seen that in order to select the optimal parameters of admixture of rubber granules, multiple graphs should be analyzed simultaneously. For example, some wave-forms reach zero values, which might seem a mistake. However, it must be taken into account that ranges of input variables (predictors) exceed limits for some output parameters. Therefore, when analyzing the results, one should look for such values of the horizontal axis, for which the strength parameters (CSC and BSC) presented on the vertical axis are as high as possible. Most often, this kind of choice will be a kind of trade off.

It can be concluded that the optimal level of admixture of rubber in CSC and BSC should not exceed 10%. In turn, the diameter of the granules should oscillate from ø 0.35 mm to ø 0.5 mm. With these parameters, the admixtures, CSC and BSC

values remain at relatively high levels. If we add to the target beam also minimizing the time of setting the gypsum mixture, the optimal mixture should contain 10% admixture with a granule diameter of ø 0.35 mm.

To analyze the increase in load bearing capacity of joints filling expansion joints a different gypsum sample size would be used. In turn, to simulate the parameters of welds in smaller building gaps, it is likely that other cross-section shapes should be used. On the basis of the research results presented above, it can be concluded that addition of polymer admixtures with different percentage to the gypsum mixture increases both the flexibility of the mortar and load transfer without damaging the weld structure, which increases the range of use of ceramic and architectural elements with such admixtures.

Further studies are required to evaluate and distinguish influence of crumb rubber inclusions from fibers' contribution, as recent studies have indicated a significant potential of recycled tire polymer fibers (RTPF) in the construction industry.

REFERENCES

Aslani, F., Ma, G., Wan, D. L. Y., & Muselin, G. (2018). Development of high-performance self-compacting concrete using waste recycled concrete aggregates and rubber granules. *Journal of Cleaner Production*, *182*, 553-566. doi:doi.org/10.1016/j.jclepro.2018.02.074

Baricevic, A., Jelcic Rukavina, M., & Pezer, M. (2018). Influence of recycled tire polymer fibers on concrete properties. *Cement and Concrete Composites*, *91*, 29–41.

Benosman, A. S., Taïbi, H., Senhadji, Y., Mouli, M., Belbachir, M., & Bahlouli, M. I. (2017). Plastic Waste Particles in Mortar Composites: Sulfate Resistance and Thermal Coefficients. *Progress in Rubber, Plastics and Recycling Technology*, *33*(3), 171.

Bergström, L., Sturm (née Rosseeva), E. V., Salazar-Alvarez, G., & Cölfen, H. (2015). Mesocrystals in biominerals and colloidal arrays. *Acc. Chem. Res.*, *48*, 1391–1402. doi:10.1021/ar500440b

Chłądzyński, S. (2008). *Spoiwa gipsowe w budownictwie*. Warsawa: Dom wydawniczy Medium.

Aciu, C. (2013). Possibilities of Recycling Rubber Waste in the Composition of Mortars. *ProEnvironment Promediu*, *6*(15).

Di Mundo, R., Petrella, A., & Notarnicola, M. (2018). Surface and bulk hydrophobic cement composites by tyre rubber addition. *Construction and Building Materials*, *172*, 176–184. doi:10.1016/j.conbuildmat.2018.03.233

Forrest, M. (2014). *Recycling and re-use of waste rubber*. Shropshire: Smithers Rapra.

Gorninski, J. P., Dal Molin, D. C., & Kazmierczak, C. S. (2007). Strength degradation of polymer concrete in acidic environments. *Cem. Concr. Compos.*, *29*(8), 637–645. doi:10.1016/j.cemconcomp.2007.04.001

Herrero, S., Mayor, P., & Hernandez-Olivarez, F. (2013). Influence of proportion and particle size gradation of rubber from end-of-life tires on mechanical, thermal and acoustic properties of plaster-rubber mortars. *Materials & Design*, *47*, 633–642. doi:10.1016/j.matdes.2012.12.063

Hooton, R. D. (2015). Current developments and future needs in standards for cementitious materials. *Cement and Concrete Research*, *78*, 165–177. doi:10.1016/j.cemconres.2015.05.022

Jafari, K., Tabatabaeian, M., Joshaghani, A., & Ozbakkaloglu, T. (2018). Optimizing the mixture design of polymer concrete: An experimental investigation. *Construction and Building Materials*, *167*, 185–196. doi:10.1016/j.conbuildmat.2018.01.191

Jarosiński, A., Żelazny, S., & Nowak, A. (2007). *Warunki otrzymywania spoiwa gipsowego z produktu odpadowego pochodzącego z procesu pozyskiwania koncentratu cynku*. Kraków: Czasopismo techniczne 1/Ch-2007 Wydawnictwo Politechniki Krakowskiej.

Konar, B., Das, A., Gupta, P. K., & Saha, M. (2011). Physicochemical characteristics of styrene-butadiene latex- modified mortar composite vis-à-vis preferential interactions. *J. Macromol. Sci.*, *48* (9), 757–765. doi:10.1080/10601325.2011.596072

Kou, S.-C., & Poon, C.-S. (2013). A novel polymer concrete made with recycled glass aggregates, fly ash and metakaolin. *Constr Build Mater.*, *41*, 146–151. doi:10.1016/j.conbuildmat.2012.11.083

Lorrentz, P. (2015). *Artificial Neural Systems: Principle and Practice*. Bentham Science Publishers. doi: 10.2174/97816810809011150101

Al Menhosh, A., Wang, Y., Wang, Y., & Augusthus-Nelson, L. (2018). Long term durability properties of concrete modified with metakaolin and polymer admixture. *Construction and Building Materials, 172*, 41–51. doi:10.1016/j.conbuildmat.2018.03.215

Osiecka, E. (2005). *Materiały budowlane – tworzywa sztuczne*. Warszawa: Oficyna Wydawnicza Politechniki Warszawskiej.

Pedro, D., De Brito, J., & Veiga, R. (2012). Mortars made with fine granulate from shredded tires. *Journal of Materials in Civil Engineering*, *25*(4), 519–529. doi:10.1061/(ASCE)MT.1943-5533.0000606

Picker, A., Nicoleau, L., Burghard, Z., Bill, J., Zlotnikov, I., Labbez, C., Nonat, A., & Cölfen, H. (2017). Mesocrystalline calcium silicate hydrate: A bioinspired route toward elastic concrete materials. *Science Advances*, *11*(3), 37–49. doi:10.1126/sciadv.1701216

Sahmaran, M., & Li, V. C. (2009). Durability properties of micro-cracked ECC containing high volumes fly ash. *Cem. Concr. Res., 39*, 1033–1043. doi:10.1016/j.cemconres.2009.07.009

Seto, J., Ma, Y., Davis, S. A., Meldrum, F., Gourrier, A., Kim, Y.-Y., Cölfen, H. (2012). Structure-property relationships of a biological mesocrystal in the adult sea urchin spine. *Proceedings of the National Academy of Sciences*, *109*(10), 3699.

Serdar, M., Baricevic, A., Jelcic Rukavina, M., Pezer, M., & Bjegovic, D. (2015). Shrinkage behaviour of fibre reinforced concrete with recycled tyre polymer fibres. *Int. J. Polym. Sci.*, 145918. doi:10.1155/2015/145918

Serna, Á., del Rio, M., Palomo, J. G., & González, M. (2012). Improvement of gypsum plaster strain capacity by the addition of rubber particles from recycled tyres. *Construction and Building Materials*, *35*, 633–641. doi:10.1016/j.conbuildmat.2012.04.093

Sosoi, G., Barbuta, M., Serbanoiu, A. A., Babor, D., & Burlacu, A. (2018). Wastes as aggregate substitution in polymer concrete. *Procedia Manufacturing, 22*, 347–351. doi: 10.1016/j.promfg.2018.03.052

Tanyildizi, H., & Asilturk, E. (2018). High temperature resistance of polymer-phosphazene concrete for 365 days. *Construction and Building Materials*, *174*, 741–748. doi:10.1016/j.conbuildmat.2018.04.078

Thomas, P., & Thomas, A. (2011). Multilayer perceptron for simulation models reduction: Application to a sawmill workshop. *Engineering Applications of Artificial Intelligence*, *24*(4), 646-657. doi:10.1016/j.engappai.2011.01.004